



Chloride-induced corrosion behavior of reinforcing steel in spent fluid cracking catalyst modified mortars

Y. Morozov^a, A.S. Castela^{a,b}, A.P.S. Dias^a, M.F. Montemor^{a,*}

^a ICEMS, DEQB, Instituto Superior Técnico, Technical University of Lisbon, Av. Rovisco Pais 1049-001 Lisboa, Portugal

^b Escola Superior de Tecnologia do Barreiro, Instituto Politécnico de Setúbal, Largo Defensores da República, 1, 2910-470 Setúbal, Portugal

ARTICLE INFO

Article history:

Received 17 April 2012

Accepted 29 January 2013

Keywords:

Reinforcing steel (D)

Mortar (E)

Corrosion (C)

Spent FCC catalyst (E)

Electrochemical impedance spectroscopy (B)

ABSTRACT

Concrete properties can be improved by various additives. Nowadays there is a strong interest concerning the use of spent fluid catalytic cracking catalyst (SFCC) as an admixture to improve mechanical properties of concrete. This work aims at studying the corrosion resistance of steel rebars in SFCC modified mortar specimens. Results of physicochemical characterization indicate the acceleration of cement hydration due to pozzolanic activity of SFCC. Electrochemical measurements show that the addition of the SFCC enhances corrosion resistance by delaying its corrosion onset and decreasing the corrosion rate. These benefits can be attributed to the reduction of the mortar permeability.

© 2013 Elsevier Ltd. All rights reserved.

1. Introduction

Corrosion of reinforcing steel is a major problem in the maintenance of the integrity of concrete structures. Steel rebars are protected against corrosion by both chemical and physical mechanisms. The chemical protection is provided by the concrete high pH (12–13), which promotes the formation of a passive film on the steel surface. On the other hand, concrete acts as a physical barrier, hindering the access of aggressive agents. However, oxygen, water, chlorides and/or carbon dioxide can be transported through concrete, reaching the rebars and inducing corrosion attack. The chloride ions, when above a threshold value, provoke a local breakdown of the passive film and pitting corrosion. Carbon dioxide, and its hydrolysis products react with the alkaline species present in concrete, leading to pH decrease to values as low as 9. In this condition the passive film is no longer stable, and the rebars enter a process of uniform corrosion. Independently of its origin, the corrosion process results in the formation of expansive corrosion products, which accumulate at the steel concrete interface, promoting cracking and, ultimately, spalling of the concrete cover [1,2].

There are several strategies to extend the lifetime of the reinforcing steel. At steel level protection can be achieved via the application of coatings (e.g. galvanized steel [1–4], organic coatings [1,2,5,6]), use of stainless steels [1,2,7–9] or cathodic protection [1,2,10,11]. Use of steel corrosion inhibitors is also a common approach [1,2,12–14]. At concrete level, the strategy normally consists on the modification of its composition with additives that enhance concrete resistivity and therefore the barrier

properties. Admixtures like fly ash [15–18], slags [18,19] and silica fume [17–20] are widely used. These additives are reported as having beneficial effects on the mechanical properties and porosity of concrete, delaying the ingress of aggressive species. Another additive that can be used for the modification of the concrete matrix is spent fluid catalytic cracking aluminosilicate catalyst (hereinafter referred SFCC), a waste from the petrochemical industry [21–24].

The utilization of SFCC in concrete production brings economic benefits because it is a low cost material that can be used to replace the higher-cost cement. This approach also provides an environmental friendly solution for the use of such industrial waste. In the 2004 the market for fresh fluid catalytic cracking catalyst was around 120 thousand tons per year with a compound annual growth rate of 4.4%; the total quantity of SFCC generated worldwide was estimated in the range of 150–170 thousand tons per year [23]. On the other hand, in 2010 the annual world production of hydraulic cement was 3300 million tons [25]. Therefore the application of SFCC as an admixture in a reasonable amount to all cement produced is hardly possible; however it can be used in cases when enhanced characteristics of the concrete are necessary. Most of the literature is focussed on the compatibility of the SFCC with concrete with emphasis on the resulting mechanical properties. According to literature, SFCC shows pozzolanic activity [26–32] and contributes for the acceleration of the hydration and setting processes [27]. SFCC addition also increases the compressive and flexural strength [22,28,33] and decreases the porosity of concrete [29,32]. However, studies focussed on the effect of SFCC on the electrochemical behavior of the rebars are scarce. Pacewska et al. [29] have investigated the role of these additives and found that in addition to beneficial effects on the mechanical properties, they do not deteriorate the steel passivation ability of concrete when used as a 10% additive, but at a content of 20 wt.%, it can make difficult the formation of a passive

* Corresponding author. Tel.: +351 218419771.

E-mail address: mfmontemor@ist.utl.pt (M.F. Montemor).

layer. Zornoza et al. [34] have reported that spent catalyst improves chloride binding properties of mortars.

The present work aims at contributing for the state-of-art, by evaluating the impact of SFCC on the corrosion behavior of reinforcing steels in mortar specimens. For this purpose, accelerated corrosion tests were performed using mortar samples exposed to chlorides. The use of mortar with low cover thickness provides a reliable and fast way to evaluate the corrosion behavior of steel rebars and has been reported in several papers [15,16,35,36]. It is consensual that these tests anticipate the behavior of the reinforcing steel in larger concrete samples.

The electrochemical behavior of the reinforcing steel can be studied by means of various electrochemical techniques. Open circuit potential (OCP) is one of the most used procedures for routine inspection of reinforced concrete structures [37–39], providing qualitative information. Measuring of the DC polarization resistance allows extracting quantitative data concerning the corrosion rate [1,37,39].

Electrochemical impedance spectroscopy (EIS) is a non-destructive monitoring technique that induces little perturbation on the steel electrode, being very suitable for the studies of reinforcing steel. EIS provides a wide range of quantitative information such as electrical resistivity, dielectric properties of the concrete cover, corrosion rate, properties of surface films, presence of adsorbed species and kinetic information [39–45].

2. Experimental

2.1. Mortar specimens

The materials used were Portland cement, Tagus river sand, SFCC from local petrochemical industry, and low carbon steel (composition in wt.%: C (0.35–0.45), Mn (0.6–0.9), Si (0.1–0.3), S (max. 0.05), P (max. 0.05), bal. Fe).

The SFCC is a powdered material represented by round and elliptical particles or their agglomerates with sizes ranging from 10 to 200 μm (Fig. 1), which is comparable with the size of cement grains (1–80 μm). The EDS analysis showed that SFCC is aluminosilicate with the ratio of $\text{Al}_2\text{O}_3:\text{SiO}_2$ equal to ca. 1:1.5 (mol.). The BET surface area assessed by the nitrogen adsorption at -196°C is 118 m^2/g .

The configuration of the cylindrical mortar specimens is shown in Fig. 2. Steel rebars were cut and cleaned out with silicon carbide paper up to 2400 grit size and rinsed afterwards with water and ethanol. Identical abrading procedure was implied to ensure the similar conditions for all the bars used in the experiment. A copper wire was used for electrical connection and the exposed area 18.9 cm^2 , was defined with an epoxy resin (Araldite™AralditeRapid); the thickness of the mortar cover was 0.7 cm. The mortar mixtures used in this work are depicted in Table 1: formulations with and without SFCC, with and without chloride addition were used for the accelerated corrosion tests. Duplicated

samples were prepared for all the conditions. After vibration the mortar samples were cured in a humidity chamber (95% RH, 20 $^\circ\text{C}$) for 28 days.

2.2. Electrochemical experiments

After cure, the samples were partially immersed for 5 weeks in a 3% NaCl solution, in which half of the exposed rebar was under immersion level. This was done to simulate the nature conditions occurred in reinforced concrete structures partially subjected to sea water. The mortar samples were kept in humid and aerated environment. The electrochemical measurements were carried out at room temperature in a Faraday cage. A conventional three-electrode arrangement was used, consisting of a Ti mesh radially located around the sample as counter electrode, a saturated calomel reference electrode connected with the sample by a wet sponge, and the rebar as working electrode.

The electrochemical measurements were performed using an Autolab PGSTAT302N potentiostat–galvanostat. The potentials are presented versus the standard hydrogen electrode (SHE).

The electrochemical impedance spectra were obtained using an amplitude of 10 mV (rms) versus the open circuit potential (OCP) within the frequency range from 50 kHz to 5 MHz. The impedance spectra were validated using the Kramers–Kronig (K–K) relations, to ensure causality, linearity and stability of the measurements [45]. The impedance plots were fitted within the range from 756 Hz to 5 MHz using the ZView 3.1c software.

The potentiodynamic polarization measurements were performed at the end of the immersion period (35 days) with a scan rate of 1 mV/s from -0.35 V (OCP) towards anodic potentials, until the current or potential reached 40 A/m^2 or 1.2 V (OCP), respectively.

2.3. Physicochemical analysis

The infrared spectra were collected with a resolution of 16 cm^{-1} , using FT-MIR spectrometer BOMEN (FTLA2000-100, ABB) with DTGS detector. A horizontal total attenuated reflection accessory with ZnSe crystal (PIKE Technologies) was used. 64 scans were obtained for each spectrum to optimize signal-to-noise ratio.

Thermal analysis (TG and DTG) was performed at 10 $^\circ$ /min speed from 50 to 950 $^\circ\text{C}$ in 30 ml/min flow of air using Labsys (Setaram). Thermal data were recalculated regarding to ignited weight basis [38].

The XRD patterns of powder samples were recorded at room temperature using a Rigaku Geigerflex diffractometer with Cu-K α radiation (Ni filter) at 40 kV and 40 mA with 2 θ from 5 to 80 $^\circ$ and a step of 0.025 $^\circ$ on 1 s/step scan speed.

Low temperature physical adsorption–desorption of nitrogen was studied with an analyzer of surface and porosity ASAP 2020 MP

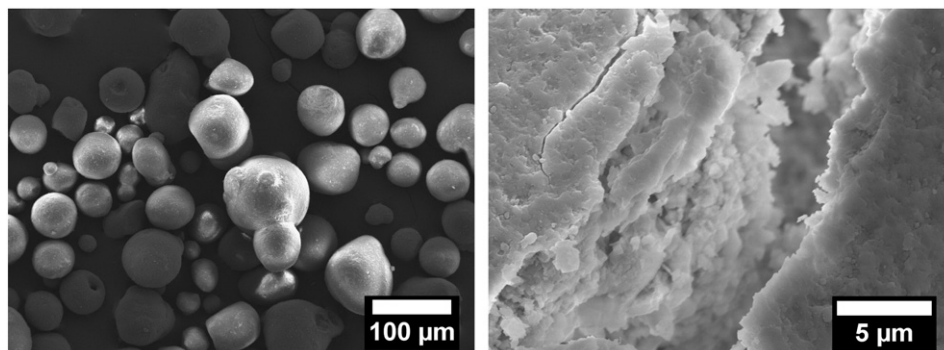


Fig. 1. SEM images of SFCC as received.

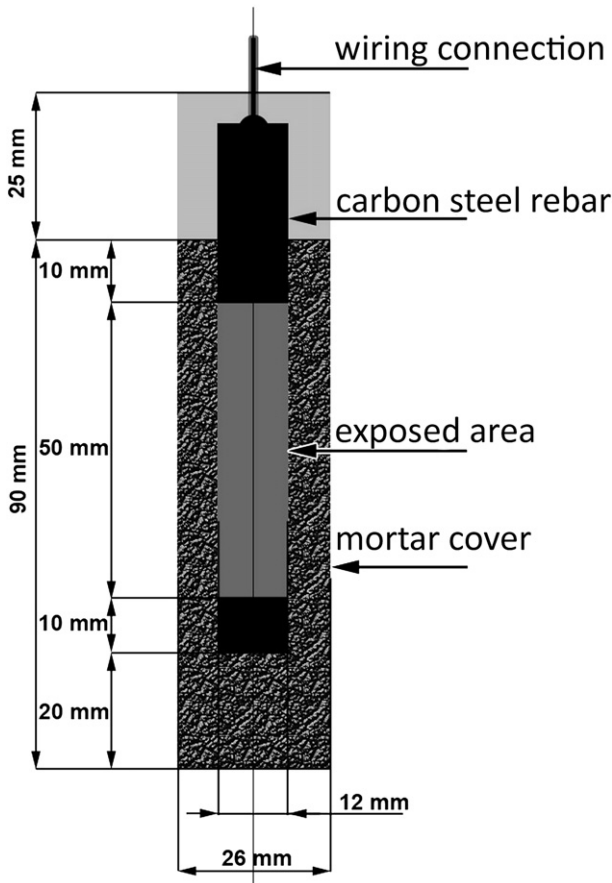


Fig. 2. The embedded steel electrode.

(Micrometrics, US). The samples were vacuumed prior measurements at 250 °C for 1 h.

3. Results and discussion

3.1. The effect of the SFCC on the composition of mortar

The XRD patterns (Fig. 3a) obtained prior immersion for the blank mortars and for the mortars with SFCC (samples I and II, respectively) indicate the presence of hydrated and non-hydrated calcium silicate (CSH and CS respectively), portlandite ($\text{Ca}(\text{OH})_2$), calcite (CaCO_3) and silica (SiO_2) phases. The peaks of hydrated calcium aluminum silicates should be detected, however they overlap with CSH and are not presented in the XRD patterns (Fig. 3a).

The FT-MIR spectra (Fig. 3b) reveal that the mortar sample with SFCC shows more intense peaks for CSH ($4000\text{--}2800, 1550\text{--}1650\text{ cm}^{-1}$) and weaker peaks for CS ($700\text{--}1200\text{ cm}^{-1}$) comparatively to the blank sample. Thus, the addition of SFCC seems to enhance the signal of the hydrated phases and therefore the mortar hydration processes.

The thermal analysis (Fig. 3c) evidences the three regions of mass loss. The first one ($50\text{--}200\text{ }^\circ\text{C}$) corresponds to the dehydration of free

water and CSH. Several overlapped peaks can be observed. According to TG data, the SFCC based mortar has higher amount of hydrated products, supporting the FT-MIR findings. The second region ($390\text{--}510\text{ }^\circ\text{C}$) is attributed to the dehydration of $\text{Ca}(\text{OH})_2$. DTG curves indicate that SFCC evidences pozzolanic activity, but the accurate quantification could not be performed. This finding agrees with previous works [26–32], which report that this additive shows pozzolanic activity. The decrease of the peak maxima ($10\text{ }^\circ\text{C}$), with the addition of SFCC, can be attributed to the reduction of $\text{Ca}(\text{OH})_2$ crystal size [46]. Sharper shift to lower temperatures ($35\text{ }^\circ\text{C}$), as well as the decrease in mass loss with the addition of SFCC, can be noticed by analyzing the third region ($650\text{--}850\text{ }^\circ\text{C}$), which corresponds to the CaCO_3 decarboxylation. However, mostly CO_2 and some carbonate peaks ($2250\text{--}2400, 1730\text{--}1780, 1350\text{--}1450\text{ cm}^{-1}$) in the FT-MIR spectra are more intense for the mortar sample with SFCC. One possible explanation is that carbon dioxide undergoes a selective adsorption on SFCC added to the mortar samples.

XRD and thermal analysis of the samples I and II performed at the end of the immersion tests are depicted in Fig. 4. Additional contribution appears in DTG curves (Fig. 4a), corresponding to the formation of Friedel's salt (FS). This peak was detected at $310\text{ }^\circ\text{C}$ (sample I) and $318\text{ }^\circ\text{C}$ (sample II), as shown by XRD at 11.1° (Fig. 4b). The thermal analysis shows that SFCC modified mortar is characterized by the higher

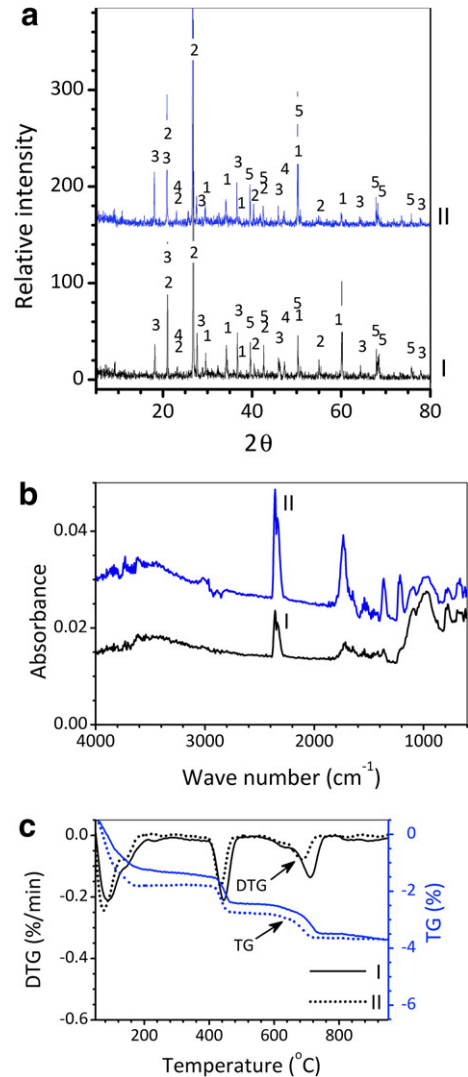


Fig. 3. Characterization of blank mortar (I) and mortar with 15% replacement of cement by SFCC (II): (a) the XRD patterns: 1 – CS-phases, 2 – CSH-phases, 3 – portlandite phases, 4 – calcite, 5 – silica phases; (b) FT-MIR spectra; (c) TG/DTG results.

Table 1
The composition of the mortars.

Sample designation	Liquid phase	SFCC
Blank, H ₂ O (I)	Distilled water	No addition
SFCC, H ₂ O (II)	Distilled water	15% replacement of cement
Blank, Cl ⁻ (III)	3% NaCl solution	no addition
SFCC, Cl ⁻ (IV)	3% NaCl solution	15% replacement of cement

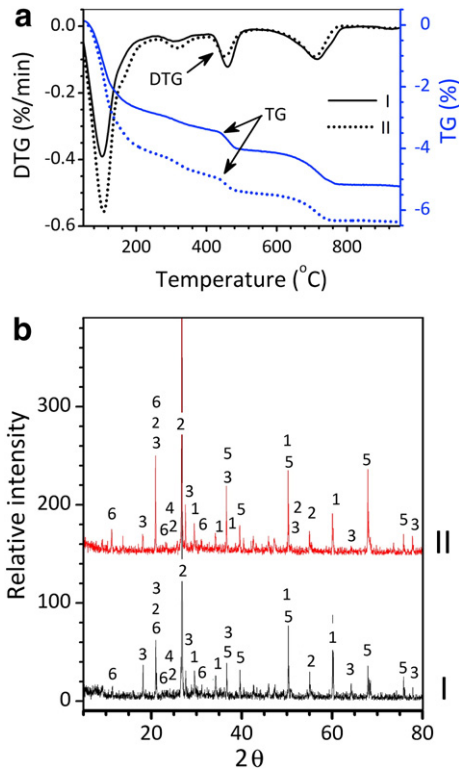


Fig. 4. Characterization of blank mortar (I) and mortar with 15% replacement of cement by SFCC (II) after the immersion test: (a) TG/DTG results; (b) the XRD patterns: 1 – CS-phases, 2 – CSH-phases, 3 – portlandite phases, 4 – calcite, 5 – silica phases, 6 – calcium silicate hydroxide chloride (FS).

concentrations of FS. The increased chloride binding ability and the resulting higher chloride threshold was also reported elsewhere [31,34].

The comparison of the TG/DTG curves before and after immersion in NaCl solutions shows that the first peak (50–200 °C) increased more than twice, mainly due to the water, which can be revealed by the shift of the global minimum on DTG curve to lower temperatures. The amount of $\text{Ca}(\text{OH})_2$ decreased twice. The corresponding DTG peaks are more than 10 °C lower, pointing a decrease in the crystal size. Unlike $\text{Ca}(\text{OH})_2$, the CaCO_3 peaks remain unchanged, indicating that the aging in the immersion solution was not affected by the carbonation process.

3.2. Electrochemical behavior of the reinforcing steel

The evolution of the open circuit potential (OCP) of the steel rebars embedded in mortar for the various compositions is presented in the Fig. 5. Samples I and II reveal the most positive potential values during the early stages of immersion. However, after a certain time, the potential starts to decrease, suggesting corrosion onset. This happens after approximately 1 and 3 weeks of immersion, respectively, for samples I and II. Such behavior clearly indicates that the presence of SFCC delays the time necessary for corrosion initiation. However, for samples III and IV, the potential values decrease gradually from the early stages of immersion indicating that rebars' depassivation occurs much earlier, since the mortar was contaminated with chlorides in the mixture phase. The OCP values are very similar and follow the same trend, thus revealing that SFCC does not affect the OCP evolution for samples III and IV. After 4 weeks all the samples showed potential values below -300 mV (SHE), revealing active corrosion processes. Therefore, according to the OCP measurements, SFCC contributes to decrease the access of chloride to the rebars, thus extending the passivation period in the mortar mixtures without chloride addition at the preparation phase.

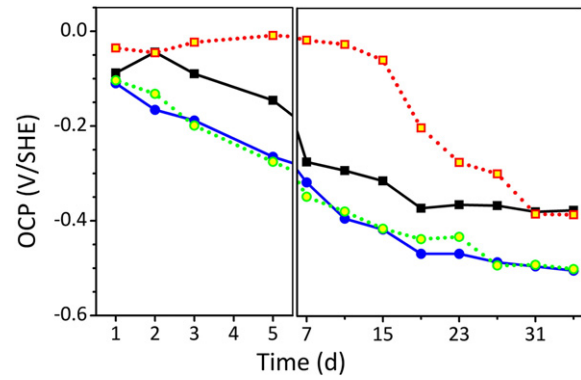


Fig. 5. OCP evolution of the steel electrode embedded in mortar samples immersed in a 3% NaCl solution.

Electrochemical impedance (EIS) was used to extract electrochemical quantitative information. Fig. 6 shows the impedance spectra after 3, 15 and 35 days of immersion. The high frequency response can be attributed to the interstitial mortar electrolyte and increases with time, indicating an enhancement of the mortar resistivity. The mid- and low frequency response is characteristic of the steel/concrete interface and can be correlated with the corrosion activity.

For early stages of immersion the EIS evolution reveals a capacitive response for samples I and II; the effect being more pronounced in sample II. For sample I, the impedance values show a significant drop after 7 days of immersion whereas for sample II the capacitive trend can be observed until 3 weeks of immersion. This points out that the presence of SFCC delays rebars depassivation in agreement with the OCP evolution.

Samples III and IV revealed the lowest impedance values since the early stages of immersion. This result was expected due to the contamination of the mortar mixture with chlorides in the preparation phase. The low frequency impedance values are about one order of magnitude lower than the ones measured for samples I and II and no relevant differences could be observed between the blank mortar and the SFCC containing mortar (III and IV, respectively). This result also agrees with the OCP observations.

At later stages (4–5 weeks) of immersion, all the samples showed similar impedance values in the low frequency range. The evolution of the phase angle plot, which starts to reveal a low frequency tail accounted for the presence of phenomena characterized by low relaxation times, most probably processes controlled by mass diffusion kinetics.

Decoupling of the various electrochemical parameters can be performed by fitting the EIS spectra. Various equivalent electrical circuit models can be used to fit the experimental data, but the one illustrated in Fig. 7 was selected in this work for the EIS analysis. Since the dispersion effects and semi-circle depression are very common phenomena in experimental EIS data [45], constant phase elements (CPE) were used instead of capacitors.

Theoretically, three main current paths can be outlined in the concrete/mortar cover: (i) continuous conductive path (CCP), corresponding to the crossing pores, and assigned to a resistance R_{CCP} ; (ii) discontinuous conductive paths (DCP) resulting from occluded pores, or pores, whose continuity is blocked by the cement paste layers referred to as the points of discontinuity (DP), described by resistance R_{CP} and capacitance C_{DP} in series; and (iii) insulating path (IP) assigned to gel particles and stony aggregates, represented by capacitance C_{IP} and resistance R_{IP} in parallel. The dielectric properties of the concrete/mortar cover should result in two capacitive loops in the Nyquist plot in the high frequency range (> 100 kHz) [47,48]. In this work these effects are hardly visible due to instrumentation limitations and small mortar cover used. The response from the steel can be described by the conventional circuit presented elsewhere [49,50]. Therefore, the equivalent circuit used for fitting is composed of the following electrical elements: in the high frequency range, the resistor R_{ir} accounts for the resistive contribution of

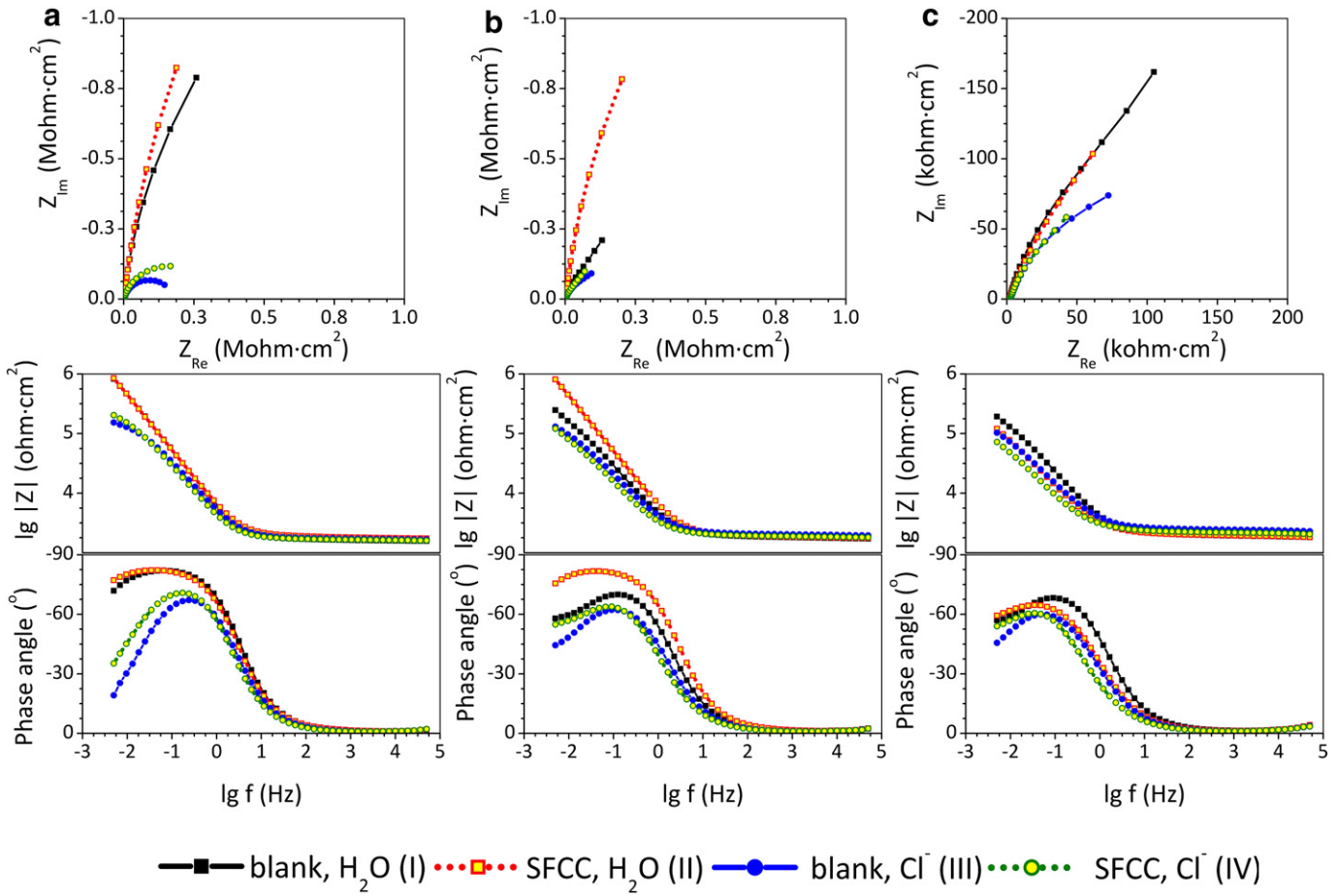


Fig. 6. Impedance spectra (Nyquist and Bode plots) after (a) 3, (b) 15 and (c) 35 days of immersion.

the electrolyte in the mortar pores; R_{ox} and CPE_{ox} , can be attributed to passive film resistance and capacitance, respectively; R_{ct} and CPE_{dl} , account for charge transfer resistance and double layer capacitance. Finally, CPE_d was included in order to simulate the contribution of diffusion phenomena occurring at low frequencies. The average values of the resistive and dielectric parameters extracted by fitting are given in Fig. 8 and Table 2, respectively.

The R_{ox}/CPE_{ox} association accounts for the response of the protective surface film. At the beginning of the immersion R_{ox} values (Fig. 8a) are similar for all the samples and it is not possible to correlate it with the presence of SFCC. However, the sample II tends to present higher values of electrical resistance up to approximately 2 weeks of immersion. At the end of the immersion test, all samples showed a decrease of R_{ox} and the values are all in the same range. The CPE_{ox} values are listed in the Table 2. The decrease of CPE exponential factor, alpha (α), (from above 0.9 to 0.8–0.85) can be associated to a more heterogeneous steel surface with more defects in the passive film, an effect that appears more evidenced for the samples contaminated with chloride during the preparation phase.

The charge transfer resistance, R_{ct} (Fig. 8b) is one of the most informative parameters, since it is inversely proportional to the corrosion rate of the steel rebars. For samples III and IV the R_{ct} values are close and decrease gradually with the immersion time. Concerning the effect

of SFCC no relevant differences were noticed, confirming that in chloride contaminated mortar the addition of SFCC has neither beneficial nor negative impact in the rebar corrosion activity. Contrarily, for samples I and II, the beneficial effects of SFCC are clearly reflected in the R_{ct} evolution. During the first week of immersion both samples show values above $1 \text{ M}\Omega \cdot \text{cm}^2$, confirming that the steel is in the passive state. For sample I, after the first week, there is a drop of R_{ct} indicating corrosion onset. After that the values gradually decreased until the end of the immersion test, attaining values similar to samples III and IV. This is consistent with the accumulation of chlorides at the mortar/rebar interface and consequent corrosion activity.

Sample II shows the highest R_{ct} values ($3\text{--}8 \text{ M}\Omega \cdot \text{cm}^2$) that keep approximately constant during the first three weeks of immersion. After this period, and in agreement with the OCP evolution, there is a gradual decrease of R_{ct} with stabilization around $0.7\text{--}0.9 \text{ M}\Omega \cdot \text{cm}^2$ at the end of the immersion tests. These values are more than 3 times higher than the ones determined for the other three samples, pointing out the protective role that SFCC exerts on the reinforcing steel. Therefore, in mortar samples without chloride contamination of the fresh mix there are two major effects arising from the presence of SFCC: delay of corrosion onset (related to passivation enhancement) and, after depassivation, lower corrosion activity.

The CPE_{dl} values (Table 2) are comparable for all the samples in the beginning of the immersion test, and there is a general tendency to increased values, which can indicate an increase of the active area at the metal–solution interface and more heterogeneous electrode surfaces. For longer immersion times the highest CPE_{dl} values and the lowest exponent factors ($\alpha - \alpha$) were measured for samples III and IV, the ones heavily contaminated with chlorides, which confirms that in these samples intense and more heterogeneous corrosion activity is

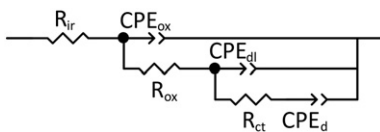


Fig. 7. Equivalent circuit model used for fitting the EIS spectra.

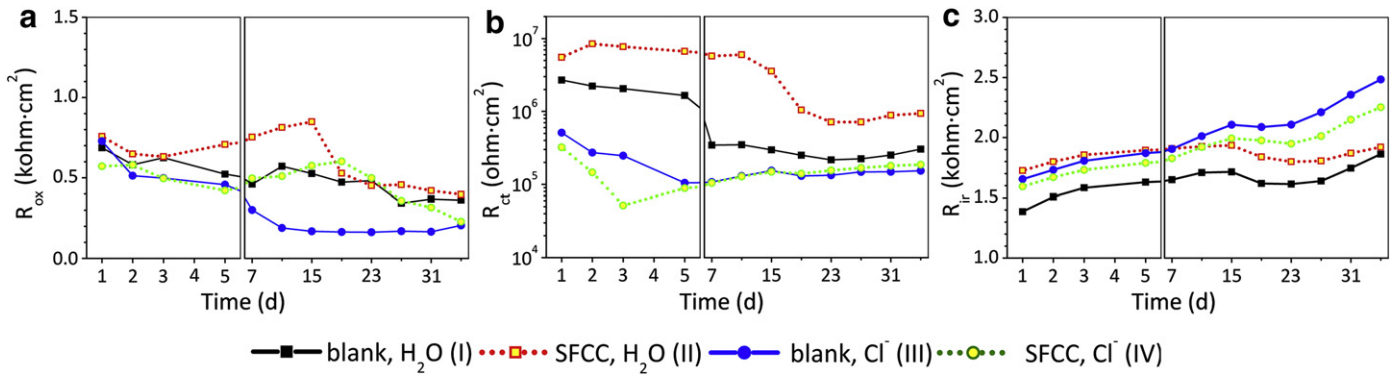


Fig. 8. Resistive parameters estimated by fitting: (a) R_{ox} , (b) R_{ct} and (c) R_{ir} .

occurring. The CPE_d values increase with time, because the diffusional control becomes progressively more significant; the effect is more relevant for samples III and IV. The results suggest that samples I and II, at early immersion times, do not present diffusion phenomena contrarily to samples III and IV. However, for longer immersion times the diffusion related phenomena start to emerge also in samples I and II, indicating a delay in the diffusion controlled phenomena response and probably the lowered amounts of corrosion products compared with the chloride contaminated samples III and IV.

The evolution of R_{ir} is depicted in the Fig. 8c. Since the conductivity of the solution, measured by the conductivity meter, was relatively constant (ca. 50 mS/cm), the changes in R_{ir} are determined by the internal changes of mortar. The R_{ir} values showed that a gradual increase for all the samples account for an increase of the concrete resistivity due to the evolution of the hydration and pozzolanic reactions.

During the early stages of immersion, the values were almost identical. However, sample II showed slightly higher R_{ir} values, suggesting that the addition of the SFCC results in more dense and less permeable mortar cover. The samples with the highest corrosion rate (with the lowest R_{ct} and OCP values) show the highest increase in R_{is} . The most plausible explanation involves the accumulation of corrosion products, which block the conductive pathways at the mortar/steel interfaces, thus increasing the electrical resistance.

Table 2
CPE parameters estimated by fitting.

Fitted element	Sample	Parameter	Time, d		
			1	7	23
CPE_{ox}	Blank, H ₂ O (I)	CPE, $\mu S \cdot cm^{-2} \cdot s^\alpha$	19	20	28
		α -Parameter	0.94	0.91	0.88
	SFCC, H ₂ O (II)	CPE, $\mu S \cdot cm^{-2} \cdot s^\alpha$	12	14	16
		α -Parameter	0.97	0.94	0.93
	Blank, Cl ⁻ (III)	CPE, $\mu S \cdot cm^{-2} \cdot s^\alpha$	19	24	25
		α -Parameter	0.91	0.86	0.78
SFCC, Cl ⁻ (IV)	CPE, $\mu S \cdot cm^{-2} \cdot s^\alpha$	23	31	38	
	α -Parameter	0.95	0.88	0.84	
CPE_{dl}	Blank, H ₂ O (I)	CPE, $\mu S \cdot cm^{-2} \cdot s^\alpha$	14	24	31
		α -Parameter	0.90	0.87	0.84
	SFCC, H ₂ O (II)	CPE, $\mu S \cdot cm^{-2} \cdot s^\alpha$	19	17	38
		α -Parameter	0.90	0.91	0.84
	Blank, Cl ⁻ (III)	CPE, $\mu S \cdot cm^{-2} \cdot s^\alpha$	13	27	78
		α -Parameter	0.87	0.81	0.74
SFCC, Cl ⁻ (IV)	CPE, $\mu S \cdot cm^{-2} \cdot s^\alpha$	19	35	55	
	α -Parameter	0.91	0.84	0.81	
CPE_d	Blank, H ₂ O (I)	CPE, $\mu S \cdot cm^{-2} \cdot s^\alpha$	-	40	30
		α -Parameter	-	0.17	0.47
	SFCC, H ₂ O (II)	CPE, $\mu S \cdot cm^{-2} \cdot s^\alpha$	-	-	3
		α -Parameter	-	-	0.32
	Blank, Cl ⁻ (III)	CPE, $\mu S \cdot cm^{-2} \cdot s^\alpha$	24	59	197
		α -Parameter	0.31	0.39	0.64
SFCC, Cl ⁻ (IV)	CPE, $\mu S \cdot cm^{-2} \cdot s^\alpha$	16	25	111	
	α -Parameter	0.21	0.46	0.72	

The comparison of the potentiodynamic polarization curves (Fig. 9), performed at the end of the immersion tests reveals that mortar samples with SFCC present higher anodic current densities, when compared to the respective samples without SFCC, this is particular visible for sample II. The presence of SFCC also shifts the corrosion potential towards more anodic values. This trend suggests that the steel rebars in such media presents an enhanced passivation behavior. Sample II shows the lowest corrosion current density value – approximately $3 \mu A/m^2$.

Thus, the potentiodynamic polarization results account for the beneficial role of SFCC in mortars without chloride contamination, corroborating the previous electrochemical measurements.

The electrochemical results reveal a good agreement, pointing out that the addition of SFCC in mortar samples prepared without chlorides leads to improved corrosion resistance. It is also worth noticing that in mortar samples initially contaminated with chlorides, the presence of SFCC does not present neither negative nor significant positive effects over the corrosion behavior of the steel. The EIS data shows that the addition of SFCC leads to a slight increase of the high frequency resistance, suggesting denser and less permeable mortar microstructure, originated by the higher amount of CSH gel formed due to pozzolanic reaction involving SFCC, which is confirmed by the XRD, FT-MIR and TG/DTG data.

The results obtained in this work highlight the effect of SFCC addition in mortar mixtures and present a detailed electrochemical study in which the beneficial effects of SFCC are pointed out: delay of the corrosion onset and decrease of the corrosion activity in mortar mixtures exposed to chloride environments.

4. Conclusions

Accelerated corrosion tests were performed on reinforced mortar samples with and without the addition of spent fluid catalytic cracking catalyst (SFCC). The results of the electrochemical measurements, namely open circuit potential and electrochemical impedance, show that corrosion initiation for samples with 15% substitution of cement powder with SFCC, without chlorides in the fresh mixture, is delayed for more than three times. The chloride free mortar mixtures modified with SFCC show much higher charge transfer resistance values, revealing that SFCC enhances reinforcing steel protection and decreases the corrosion rate when the steel becomes active. For samples contaminated with NaCl in the mixture preparation phase, which revealed corrosion activity since the early stages of immersion, neither beneficial nor detrimental effects of SFCC addition could be drawn concerning the corrosion resistance of the rebars.

The beneficial role of SFCC concerning the delay of the corrosion activity can be explained by the pozzolanic reactions involving SFCC that result in higher amount of calcium silica hydrated gel, proved by XRD, FT-MIR and TG/DTG data, making the concrete less permeable towards chlorides.

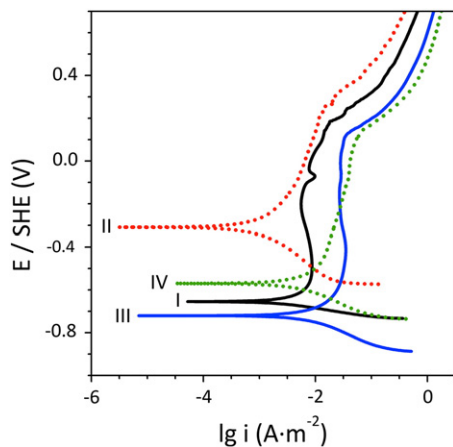


Fig. 9. DC potentiodynamic polarization curves after 35 days of immersion.

Acknowledgments

The authors are grateful to the Portuguese Foundation for Science and Technology (PTDC/ECM/105427/2008) for the financing of the research and GALP Energia for providing the spent FCC catalyst.

References

- J.P. Broomfield, *Corrosion of Steel in Concrete: Understanding, Investigation, and Repair*, E & FN Spon, 1997.
- P. Roberge, *Handbook of Corrosion Engineering*, McGraw-Hill Companies, Incorporated, 1999.
- M. Sánchez, M.C. Alonso, P. Cecílio, M.F. Montemor, C. Andrade, Electrochemical and analytical assessment of galvanized steel reinforcement pre-treated with Ce and La salts under alkaline media, *Cem. Concr. Compos.* 28 (2006) 256–266.
- S.R. Yeomans, *Galvanized Steel Reinforcement in Concrete*, Elsevier, 2004.
- A.U. Malik, I. Andijani, S. Ahmed, F. Al-Muaili, Corrosion and mechanical behavior of fusion bonded epoxy (FBE) in aqueous media, *Desalination* 150 (2002) 247–254.
- J.J. Assaad, C.A. Issa, Bond strength of epoxy-coated bars in underwater concrete, *Constr. Build. Mater.* 30 (2012) 667–674.
- L. Freire, M.J. Carmezim, M.G.S. Ferreira, M.F. Montemor, The passive behaviour of AISI 316 in alkaline media and the effect of pH: a combined electrochemical and analytical study, *Electrochim. Acta* 55 (2010) 6174–6181.
- L. Freire, M.J. Carmezim, M.G.S. Ferreira, M.F. Montemor, The electrochemical behaviour of stainless steel AISI 304 in alkaline solutions with different pH in the presence of chlorides, *Electrochim. Acta* 56 (2011) 5280–5289.
- M.C. García-Alonso, M.L. Escudero, J.M. Miranda, M.L. Vega, F. Capilla, M.J. Correia, M. Salta, A. Bennani, J.A. González, Corrosion behaviour of new stainless steels reinforcing bars embedded in concrete, *Cem. Concr. Res.* 37 (2007) 1463–1471.
- P. Pedeferrri, Cathodic protection and cathodic prevention, *Constr. Build. Mater.* 10 (1996) 391–402.
- W. Baeckmann, W. Schwenk, W. Prinz, *Handbook of Cathodic Corrosion Protection: Theory and Practice of Electrochemical Protection Processes*, Gulf Pub. Co., 1997.
- H.E. Jamil, A. Shriiri, R. Boulif, C. Bastos, M.F. Montemor, M.G.S. Ferreira, Electrochemical behaviour of amino alcohol-based inhibitors used to control corrosion of reinforcing steel, *Electrochim. Acta* 49 (2004) 2753–2760.
- H.E. Jamil, A. Shriiri, R. Boulif, M.F. Montemor, M.G.S. Ferreira, Corrosion behaviour of reinforcing steel exposed to an amino alcohol based corrosion inhibitor, *Cem. Concr. Compos.* 27 (2005) 671–678.
- M. Ormellese, L. Lazzari, S. Goidanich, G. Fumagalli, A. Brenna, A study of organic substances as inhibitors for chloride-induced corrosion in concrete, *Corros. Sci.* 51 (2009) 2959–2968.
- M.F. Montemor, A.M.P. Simões, M.M. Salta, Effect of fly ash on concrete reinforcement corrosion studied by EIS, *Cem. Concr. Compos.* 22 (2000) 175–185.
- M.F. Montemor, M.P. Cunha, M.G. Ferreira, A.M. Simões, Corrosion behaviour of rebars in fly ash mortar exposed to carbon dioxide and chlorides, *Cem. Concr. Compos.* 24 (2002) 45–53.
- U.M. Angst, B. Elsener, C.K. Larsen, Ø. Vennesland, Chloride induced reinforcement corrosion: electrochemical monitoring of initiation stage and chloride threshold values, *Corros. Sci.* 53 (2011) 1451–1464.
- V.S. Ramachandran, *Concrete Admixtures Handbook (Properties, Science and Technology)*, Standard Publishers Distributors, 2001.
- R. Siddique, J. Klaus, Influence of metakaolin on the properties of mortar and concrete: a review, *Appl. Clay Sci.* 43 (2009) 392–400.
- N. Neithalath, J. Jain, Relating rapid chloride transport parameters of concretes to microstructural features extracted from electrical impedance, *Cem. Concr. Res.* 40 (2010) 1041–1051.
- E. Furimsky, Spent refinery catalysts: environment, safety and utilization, *Catal. Today* 30 (1996) 223–286.
- N. Su, H.-Y. Fang, Z.-H. Chen, F.-S. Liu, Reuse of waste catalysts from petrochemical industries for cement substitution, *Cem. Concr. Res.* 30 (2000) 1773–1783.
- M. Marafi, A. Stanislaus, Spent catalyst waste management: a review: part I – developments in hydroprocessing catalyst waste reduction and use, *Resour. Conserv. Recycl.* 52 (2008) 859–873.
- H. Al-Dhamri, K. Melghit, Use of alumina spent catalyst and RFCC wastes from petroleum refinery to substitute bauxite in the preparation of Portland clinker, *J. Hazard. Mater.* 179 (2010) 852–859.
- H.G.v. Oss, U.S. Geological Survey, mineral commodity summaries – cement, <http://minerals.usgs.gov/minerals/pubs/commodity/cement/mcs-2011-cemen.pdf> 2011.
- S.Y.N. Chan, X. Ji, Comparative study of the initial surface absorption and chloride diffusion of high performance zeolite, silica fume and PFA concretes, *Cem. Concr. Compos.* 21 (1999) 293–300.
- B. Pacewska, I. Wilinska, M. Bukowska, W. Nocun-Wczelik, Effect of waste aluminosilicate material on cement hydration and properties of cement mortars, *Cem. Concr. Res.* 32 (2002) 1823–1830.
- Y.-S. Tseng, C.-L. Huang, K.-C. Hsu, The pozzolanic activity of a calcined waste FCC catalyst and its effect on the compressive strength of cementitious materials, *Cem. Concr. Res.* 35 (2005) 782–787.
- B. Pacewska, M. Bukowska, I. Wilinska, M. Swat, Modification of the properties of concrete by a new pozzolan – a waste catalyst from the catalytic process in a fluidized bed, *Cem. Concr. Res.* 32 (2002) 145–152.
- J. Payá, J. Monzó, M.V. Borrachero, S. Velázquez, Evaluation of the pozzolanic activity of fluid catalytic cracking catalyst residue (FC3R). Thermogravimetric analysis studies on FC3R-Portland cement pastes, *Cem. Concr. Res.* 33 (2003) 603–609.
- E. Zornoza, P. Garcés, J. Payá, M.A. Climent, Improvement of the chloride ingress resistance of OPC mortars by using spent cracking catalyst, *Cem. Concr. Res.* 39 (2009) 126–139.
- E. Zornoza, J. Payá, J. Monzó, M.V. Borrachero, P. Garcés, The carbonation of OPC mortars partially substituted with spent fluid catalytic catalyst (FC3R) and its influence on their mechanical properties, *Constr. Build. Mater.* 23 (2009) 1323–1328.
- J. Payá, J. Monzó, M.V. Borrachero, Fluid catalytic cracking catalyst residue (FC3R): an excellent mineral by-product for improving early-strength development of cement mixtures, *Cem. Concr. Res.* 29 (1999) 1773–1779.
- E. Zornoza, J. Payá, P. Garcés, Chloride-induced corrosion of steel embedded in mortars containing fly ash and spent cracking catalyst, *Corros. Sci.* 50 (2008) 1567–1575.
- C. Monticelli, A. Frignani, G. Trabonelli, A study on corrosion inhibitors for concrete application, *Cem. Concr. Res.* 30 (2000) 635–642.
- P. Garcés, L.G. Andión, E. Zornoza, M. Bonilla, J. Payá, The effect of processed fly ashes on the durability and the corrosion of steel rebars embedded in cement-modified fly ash mortars, *Cem. Concr. Compos.* 32 (2010) 204–210.
- N.S. Berke, *Techniques to Assess the Corrosion Activity of Steel Reinforced Concrete Structures*, ASTM, 1996.
- V.S. Ramachandran, J.J. Beaudoin, *Handbook of Analytical Techniques in Concrete Science and Technology: Principles, Techniques, and Applications*, Noyes Publications, 2001.
- M.F. Montemor, A.M.P. Simões, M.G.S. Ferreira, Chloride-induced corrosion on reinforcing steel: from the fundamentals to the monitoring techniques, *Cem. Concr. Compos.* 25 (2003) 491–502.
- P. Lay, P.F. Lawrence, N.J.M. Wilkins, D.E. Williams, An a.c. impedance study of steel in concrete, *J. Appl. Electrochem.* 15 (1985) 755–766.
- P. Lambert, C. Page, P. Vassie, Investigations of reinforcement corrosion. 2. Electrochemical monitoring of steel in chloride-contaminated concrete, *Mater. Struct.* 24 (1991) 351–358.
- D.D. Macdonald, M.C.H. Mckubre, M. Urquidí-Macdonald, Theoretical assessment of AC impedance spectroscopy for detecting corrosion of rebar in reinforced concrete, *Corrosion* 44 (1988) 2–7.
- K.K. Sagoe-Crentsil, F.P. Glasser, J.T.S. Irvine, Electrochemical characteristics of reinforced concrete corrosion as determined by impedance spectroscopy, *Br. Corros. J.* 27 (1992) 113–119.
- O. Poupard, A. Ait-Mokhtar, P. Dumargue, Corrosion by chlorides in reinforced concrete: determination of chloride concentration threshold by impedance spectroscopy, *Cem. Concr. Res.* 34 (2004) 991–1000.
- E. Barsouk, J.R. Macdonald, *Impedance Spectroscopy, Theory, Experiment, and Applications*, 2nd ed., John Wiley & Sons, Inc., 2005.
- T. Sato, J.J. Beaudoin, V.S. Ramachandran, L.D. Mitchell, P.J. Tumidajski, Thermal decomposition of nanoparticulate Ca(OH)₂-anomalous effects, *Adv. Cem. Res.* 19 (2007) 1–7.
- G. Song, Equivalent circuit model for AC electrochemical impedance spectroscopy of concrete, *Cem. Concr. Res.* 30 (2000) 1723–1730.
- N. Neithalath, J. Weiss, J. Olek, Characterizing enhanced porosity concrete using electrical impedance to predict acoustic and hydraulic performance, *Cem. Concr. Res.* 36 (2006) 2074–2085.
- S. Joiret, M. Keddah, X.R. Nóvoa, M.C. Pérez, C. Rangel, H. Takenouti, Use of EIS, ring-disk electrode, EQCM and Raman spectroscopy to study the film of oxides formed on iron in 1 M NaOH, *Cem. Concr. Compos.* 24 (2002) 7–15.
- M. Sánchez, J. Gregori, C. Alonso, J.J. García-Jareño, H. Takenouti, F. Vicente, Electrochemical impedance spectroscopy for studying passive layers on steel rebars immersed in alkaline solutions simulating concrete pores, *Electrochim. Acta* 52 (2007) 7634–7641.